2,3-Substituted quinoxalin-6-amine analogs as antiproliferatives: A structure activity relationship study

Qianyi Chen[a,c], **Vashti C. Bryant**[a,c], **Hernando Lopez**[a], **David L. Kelly**[a], **Xu Luo**[a], and **Amarnath Natarajan**[a,b,c,*]

[a] Eppley Institute for Cancer Research, University of Nebraska Medical Center, Omaha NE 68198

[b] Department of Genetics Cell Biology and Anatomy, University of Nebraska Medical Center, Omaha NE 68198

[c] Chemical Biology Program, Department of Pharmacology and Toxicology, University of Texas Medical Branch, Galveston TX 77555

Abstract

The quinoxaline core is considered a privileged scaffold as it is found in a variety of biologically relevant molecules. Here we report the synthesis of a quinoxalin-6-amine library, screening against a panel of cancer cell lines and a structure activity relationship (SAR). This resulted in the identification of a bisfuranylquinoxalineurea analog (**7c**) that has low micromolar potency against the panel of cancer cell lines. We also show that cells treated with quinoxalineurea **7c** results in caspase 3/7 activation, PARP cleavage and Mcl-1 dependent apoptosis.

Keywords

Quinoxaline urea; Antiproliferative; Mcl-1 dependent apoptosis

The definition of privileged scaffold has evolved over the past two decades from ligands for a diverse array of receptors to multiple compounds with similar core structure having biological activity.[1] Quinoxaline is an important class of nitrogen containing heterocycle that is found in drugs (Figure 1) that aid in smoking cessation (Varenicline), have antiglaucoma activity (Brimonidine) and have antibacterial properties (Quinacillin).[2−4] Not surprisingly, recent high throughput screening (HTS) campaigns against a variety of biological targets have identified quinoxaline analogs as hits. Quinoxaline analogs have been identified as inhibitors of heparin-induced tau fibril formation, cyclophin A, kinases (p110δ of PI3 kinase, JSP-1), phosphatases (cdc25B, MAPK phosphatase-1) and isomerases (peptidyl-prolyl-*cis-trans* isomerase).[5−11] Europium and Indium complexes containing substituted quinoxalines show large fluorescence enhancement through ligand to metal transfer, which has been exploited in developing imaging agents.[12] Together these studies indicate that the quinoxaline core is a privileged scaffold.

Our lab is focused on the identification and characterization of small molecule inhibitors of protein-protein interactions.13, 14 The early onset of breast cancer gene 1 (BRCA1) contains multiple functional domains that interact with a plethora of proteins to mediate key signal transduction events that are critical for normal cellular functions. Abnormalities of BRCA1 result in the dysfunction of the corresponding signaling networks and have been implicated in the onset and progression of cancer. A HTS using a fluorescence polarization (FP) assay to identify small molecule inhibitors of the carboxy terminus domains of BRCA1 (BRCT) resulted in the identification of a quinoxalineurea as a validated hit.10 This prompted us to generate a focused chemical library to explore this scaffold as a BRCT inhibitor. The library was screened using the BRCT FP assay.15 However, this did not result in the identification of either a compound with improved potency or a discernable structure activity relationship (SAR).

Recent studies from other labs have shown that quinoxaline analogs have antiproliferative activity with μM potency against breast and prostate cancer cell lines.[16, 17] Based on these studies and the privileged scaffold status of the quinoxalines we screened our library against a panel of cancer cell lines and estimated their growth inhibitory effects. We identified a compound (**7c**) with anti-tumor activity against a panel of cancer cell lines. We also show that this compound (**7c**) was able to induce activation of caspase 3/7, poly-ADP-ribose polymerase (PARP) cleavage and Mcl-1 dependent apoptosis.

A small focused library with substitutions at the 2,3- and 6- positions on the quinoxaline core was envisioned to probe the scaffold for biological activity (Scheme 1). The various analogs and yields for the final step are summarized in Table 1. The variations at the R^1 position were methyl, furan, thiophene and phenyl groups. At the 6- position acetyl, phenylurea and tolylsulfonamide were explored in the **5** compound series. The compounds (**5a-l**) were generated from 2,3-substituted-6-aminoquinoxaline analogs (**4**, Scheme 1)[11] with the amino group functionalized with acetyl chloride, phenylisocyanate and tosylchloride respectively. The synthesis of acetylated and phenyl urea analogs (**5a-h**) was accomplished using reported methods. However reaction of the quinoxalineamine analogs (**4**) with tosyl chloride yielded rearranged, monosubstitued and disubstituted products depending on the substitution at the 2,3-positions (**5i-l**). The amines (**4a-d**) were also reacted with isothiocyanates to generate the corresponding quinoxalinylthiourea analogs (**6a-f**). In order to generate quinoxaline urea compounds (**6g-m**) with secondary amines, 2,3-substituted quinoxaline isocyanates were generated *in situ* using triphosgene and reacted with the corresponding secondary amine.

The compounds were screened in a growth inhibition assay at 20 μM over a 72 h period in a panel of cancer cell lines (lung-A549; pancreatic-Aspc1; colon-HT29; breast-MDAMB231; prostate-PC3; ovarian-SKOV3 and bone-U2OS) and the results are summarized in Table 2. In the **5** compound series only **5a**, **5b** and **5f** inhibited growth of the various cancer cell lines. This suggests that the furan substitutions at the 2,3-positions are clearly better than the other three. It also suggests that sulfonamide substitution at the 6-position is not suitable for the growth inhibitory activity. The screening results in the **6** compound series again show that all the furan compounds (**6a**, **6d**, **6h**, **6k** and **6m**) were active. It also shows that substitution at the 4-position of the phenyl thioureas plays a role in the biological activity (**6b** and **6c** vs. **6e** and **6f**). This size effect was also observed with the urea compounds from the secondary amine (**6j** vs. **6l** and **6k** vs. **6m**).

These results prompted us to synthesize four additional compounds to probe the size effect at the 4-position on a phenyl urea (**7a-d**). Evaluation of these analogs in the growth inhibition assay clearly showed a size effect and compound **7c** with bromo substituion at the 4-position was identified as the best compound. A dose-response study with compound **7c**

shows low-μM GI_{50} values against a panel of cancer cell lines (Table 3). In summary this iterative synthesis and screening effort show that the furan substitution at the 2,3-position, a urea at the 6-position and the substitutent at the *para*-position of a phenyl urea are important for the biological activity. These studies also resulted in the identification of **7c** with low-μM GI_{50} values against a panel of cancer cell lines.

Caspases are a class of cysteine proteinases that are activated during apoptosis and measuring caspase activity is often used to detect activation of apoptotic signaling. To determine if the growth inhibitory effects observed with **7c** in various cancer cell lines were a result of programmed cell death, we explored the ability of **7c** to induce caspase-3/7. Our results show that **7c** induces caspase 3/7 much more rapidly compared to the positive control (Etoposide) in MDA-MB-231 and PC3 cells (Figure 2A and B) and the induction is sustained for 72h in these cell lines.

Bcl-xL, Bcl-2 and Mcl-1 are antiapoptotic proteins that are implicated in the survival of cancer cells.[18, 19] Bad3SA is the endogenous inhibitor of Bcl-xL and Bcl-2 but not Mcl-1. Using HeLa cells that over express Bad3SA, we explored the mechanistic basis for the induction of apoptosis by **7c.** In these cell lines expression of Bad3SA is under the control of Doxycycline (Dox). The apoptosis studies carried out in this cell line are summarized in Figure 3. As with the other cancer cell lines we observe induction of caspase 3/7 and PARP cleavage by **7c** (Figure 3A and 3B respectively). We next carried out a dose response study with **7c** in untreated cells [(−) Dox] and cells treated with Dox (1 μg/mL for 3 h) to induce Bad3SA [(+) Dox]. The cells were incubated with **7c** and a positive control (DNA damaging agent Camptothecin, CPT) for 12h. Cell death was measured by counting the number of condensed nuclei. We observed a dose dependent increase in the induction of apoptosis in the (+) Dox cells, indicating that **7c** induces apoptosis in a Mcl-1 dependent manner (Figure 3C).

In summary, a focused library of 2,3-substituted quinoxalin-6-amine analogs was synthesized and evaluated in a panel of cancer cell lines for growth inhibition. The preliminary structure activity relationship (SAR) showed bis-furan substitution at the 2,3-positions was favored. A comparison of a series of linkers between the 2,3- disubstituted quinoxaline and a substituted phenyl ring showed that a urea linker was optimal for the antiproliferative activity. In addition, the size of the substituent at the 4-position of the phenyl ring was important for the activity. This led to the identification of a bisfuranylquinoxalineurea analog (**7c**) with low micromolar potency against the panel of cancer cell lines. The analog **7c** induces caspase 3/7 activation, PARP cleavage and Mcl-1 dependent apoptosis. The molecular target of compound **7c** is currently under investigation and will be reported in due course.

Supplementary Material

Refer to Web version on PubMed Central for supplementary material.

Acknowledgments

References and notes

1. Welsch ME, Snyder SA, Stockwell BR. Curr Opin Chem Biol. 2010; 14:347. [PubMed: 20303320]

2. Escobar-Chavez JJ, Merino V, Lopez-Cervantes M, Rodriguez-Cruz IM, Quintanar-Guerrero D, Ganem-Quintanar A. Curr Drug Discov Technol. 2009; 6:171. [PubMed: 19496753]

3. McLaughlin MA, Chiou GC. J Ocul Pharmacol. 1985; 1:101. [PubMed: 3916848]

4. Hugo WB, Stretton RG. Nature. 1964; 202:1217. [PubMed: 14217514]

5. Crowe A, Ballatore C, Hyde E, Trojanowski JQ, Lee VM. Biochem Biophys Res Commun. 2007; 358:1. [PubMed: 17482143]

6. Li J, Chen J, Zhang L, Wang F, Gui C, Zhang L, Qin Y, Xu Q, Liu H, Nan F, Shen J, Bai D, Chen K, Shen X, Jiang H. Bioorg Med Chem. 2006; 14:5527. [PubMed: 16682211]

7. Berndt A, Miller S, Williams O, Le DD, Houseman BT, Pacold JI, Gorrec F, Hon WC, Liu Y, Rommel C, Gaillard P, Ruckle T, Schwarz MK, Shokat KM, Shaw JP, Williams RL. Nat Chem Biol. 2010; 6:244. [PubMed: 20154668]

8. Zhang L, Qiu B, Xiong B, Li X, Li J, Wang X, Li J, Shen J. Bioorg Med Chem Lett. 2007; 17:2118. [PubMed: 17303416]

9. Johnston PA, Foster CA, Tierno MB, Shun TY, Shinde SN, Paquette WD, Brummond KM, Wipf P, Lazo JS. Assay Drug Dev Technol. 2009; 7:250. [PubMed: 19530895]

10. Simeonov A, Yasgar A, Jadhav A, Lokesh GL, Klumpp C, Michael S, Austin CP, Natarajan A, Inglese J. Anal Biochem. 2008; 375:60. [PubMed: 18158907]

11. Wang F, Chen J, Liu X, Shen X, He X, Jiang H, Bai D. Chem Pharm Bull (Tokyo). 2006; 54:372. [PubMed: 16508195]

12. Chinen LK, Galen KP, Kuan KT, Dyszlewski ME, Ozaki H, Sawai H, Pandurangi RS, Jacobs FG, Dorshow RB, Rajagopalan R. J Med Chem. 2008; 51:957. [PubMed: 18251490]

13. Kumar EA, Charvet CD, Lokesh GL, Natarajan A. Anal Biochem. 201010.1016/j.ab.2010.11.038

14. Lokesh GL, Rachamallu A, Kumar GD, Natarajan A. Anal Biochem. 2006; 352:135. [PubMed: 16500609]

15. Joseph PR, Yuan Z, Kumar EA, Lokesh GL, Kizhake S, Rajarathnam K, Natarajan A. Biochem Biophys Res Commun. 2010; 393:207. [PubMed: 20122900]

16. Grande F, Aiello F, Grazia OD, Brizzi A, Garofalo A, Neamati N. Bioorg Med Chem. 2007; 15:288. [PubMed: 17085054]

17. Gavara L, Saugues E, Alves G, Debiton E, Anizon F, Moreau P. Eur J Med Chem. 2010; 45:5520. [PubMed: 20864224]

18. Lopez H, Zhang L, George NM, Liu X, Pang X, Evans JJ, Targy NM, Luo X. J Biol Chem. 2010; 285:15016. [PubMed: 20223826]

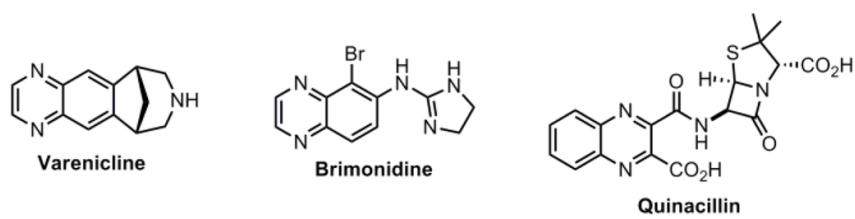19. Zhang L, Lopez H, George NM, Liu X, Pang X, Luo X. Cell Death Differ. November 26.2010 10.1038/cdd.2010.152

Figure 1.
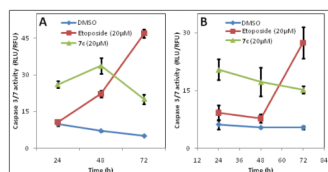Drugs containing the quinoxaline core.

Figure 2.
Induction of caspase 3/7 activity by **7c** and Etoposide (a known chemotherapeutic agent) in MDA-MB-231 breast cancer cells (A) and PC3 prostate cancer cells (B).
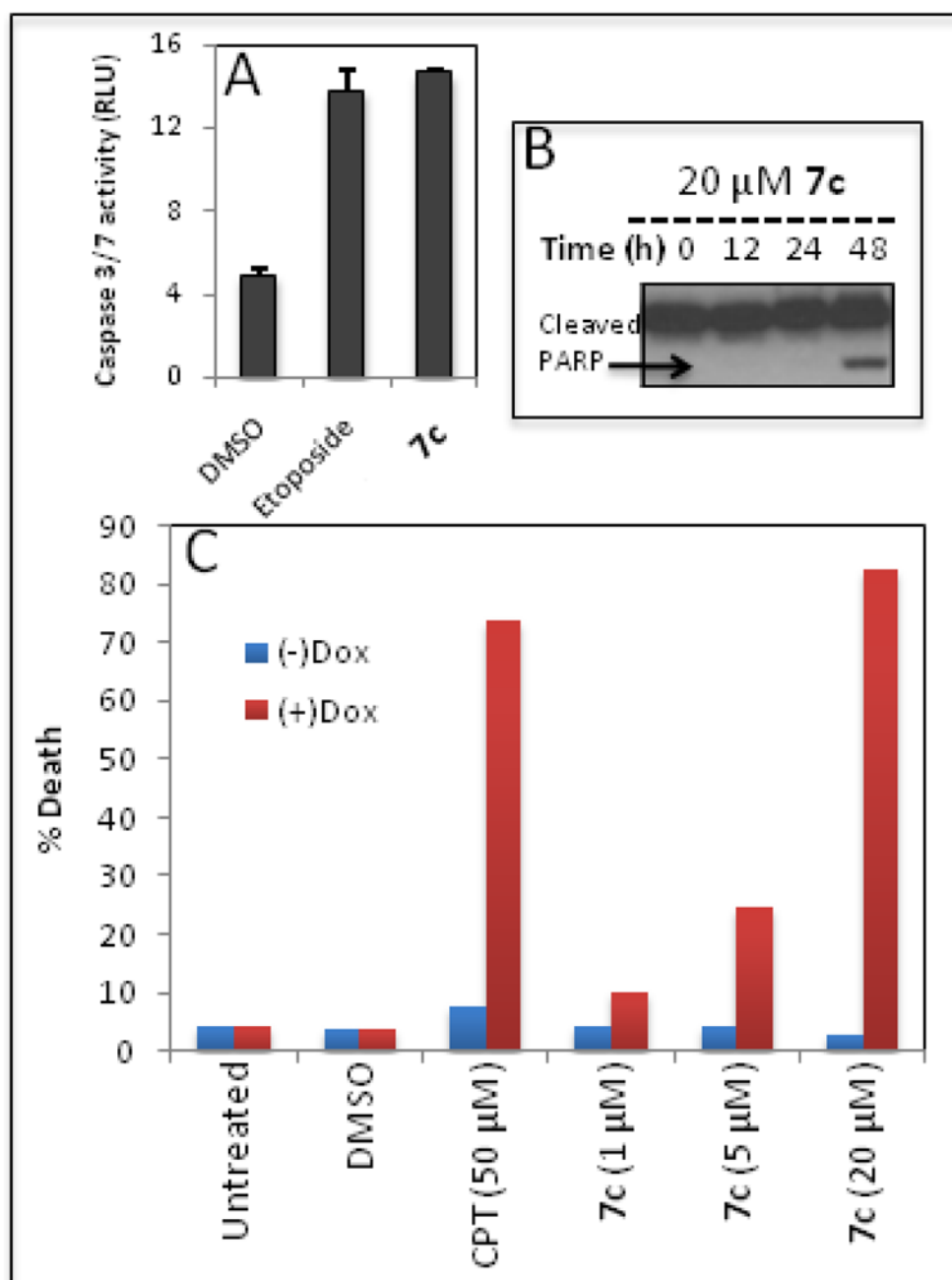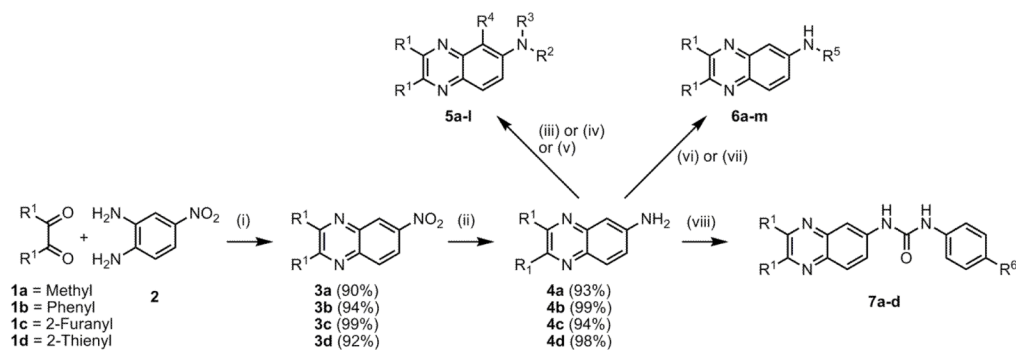
Figure 3.
Apoptosis studies in HeLa cells: (A) Induction of caspase 3/7 by **7c** and Etoposide. (B) PARP cleavage induced by **7c** assessed by Western blot. (C) Mcl-1 dependent induction of apoptosis by **7c**.

Scheme 1. Synthesis of 2,3-substituted quinoxalin-6-amine analogs
Reagents and conditions: (i) Ethanol, reflux, 36–48h; (ii) Pd/C, H_2, ethanol, room temperature, 6–8h; (iii) R^2NCO, DIPEA, DCM 24–72h; (iv) R^2COCl, DCM, 4h; (v) TsCl, TEA, DCM 6h; (vi) R^5NCS (2 eq), DCM, reflux; (vii) Triphosgene, DIPEA, DCM, 4h; Amine, DCM, 8–24h; (viii) $R^6C_6H_4NCO$ (1.5 eq), DIPEA, DCM, 12–24h.

Table 1

Isolated yields of 2,3-substituted quinoxalin-6-amine analogs.

Entry	R^1	R^2	R^3	R^4	% Isolated yield
5a	Methyl	-COCH$_3$	-H	-H	64
5b	2-Furanyl	-COCH$_3$	-H	-H	84
5c	2-Thienyl	-COCH$_3$	-H	-H	77
5d	Phenyl	-COCH$_3$	-H	-H	70
5e	Methyl	-C(=O)-NHPh	-H	-H	83
5f	2-Furanyl	-C(=O)-NHPh	-H	-H	77
5g	2-Thienyl	-C(=O)-NHPh	-H	-H	70
5h	Phenyl	-C(=O)-NHPh	-H	-H	80
5i	Methyl	-H	-H	-SO$_2$Tol	65
5j	2-Furanyl	-SO$_2$Tol	-SO$_2$Tol	-H	66
5k	2-Thienyl	-SO$_2$Tol	-SO$_2$Tol	-H	69
5l	Phenyl	-SO$_2$Tol	-H	-H	65

Entry	R^1	R^5	% Isolated yield
6a	2-Furanyl	-C(=S)-NHPh	70
6b	2-Thienyl	-C(=S)-NHPh	74
6c	Phenyl	-C(=S)-NHPh	75
6d	2-Furanyl	-C(=S)-NH-(4-Nitro)-Phenyl	78
6e	2-Thienyl	-C(=S)-NH-(4-Nitro)-Phenyl	80
6f	Phenyl	-C(=S)-NH-(4-Nitro)-Phenyl	80
6g	Methyl	-CO-Pyrrolidine	55
6h	2-Furanyl	-CO-Pyrrolidine	57
6i	Phenyl	-CO-Pyrrolidine	40
6j	Methyl	-C(=O)-NH-(4-Benzyl)-Piperidine	50
6k	2-Furanyl	-C(=O)-NH-(4-Benzyl)-Piperidine	53
6l	Methyl	-CO-Piperdine	54
6m	2-Furanyl	-CO-Morpholine	80

Entry	R^1	R^2	R^3	R^4	% Isolated yield
	R^1		R^6		
7a	2-Furanyl		-F		80
7b	2-Furanyl		-Cl		81
7c	2-Furanyl		-Br		76
7d	2-Furanyl		-Phenyl		71

Table 2

Screen results of the 2,3-substituted quinoxalin-6-amine analogs.

Entry	% Growth inhibition at 20μM						
	A549	AsPC1	HT29	MDA-MB-231	PC3	SKOV3	U2OS
5a	23.4 ± 3.3	26.2 ± 2.8	31.7 ± 2.8	25.7 ± 5.1	21.8 ± 15.1	4.0 ± 3.6	31.4 ± 3.6
5b	57.8 ± 7.0	Inactive	7.6 ± 5.1	20.3 ± 5.9	57.7 ± 9.4	9.0 ± 3.4	Inactive
5c	Inactive	Inactive	Inactive	Inactive	Inactive	Inactive	Inactive
5d	Inactive	Inactive	Inactive	Inactive	Inactive	Inactive	Inactive
5e	Inactive	Inactive	Inactive	Inactive	Inactive	Inactive	Inactive
5f	54.6 ± 2.6	9.6 ± 6.6	52.1 ± 11.6	31.3 ± 10.7	70.6 ± 1.3	24.7 ± 1.1	59.6 ± 1.6
5g	Inactive	Inactive	Inactive	Inactive	Inactive	Inactive	Inactive
5h	Inactive	Inactive	Inactive	Inactive	Inactive	Inactive	Inactive
5i	Inactive	Inactive	Inactive	Inactive	Inactive	Inactive	Inactive
5j	Inactive	Inactive	Inactive	Inactive	Inactive	Inactive	Inactive
5k	Inactive	Inactive	Inactive	Inactive	Inactive	Inactive	Inactive
5l	Inactive	Inactive	Inactive	Inactive	Inactive	Inactive	Inactive
6a	18.0 ± 0.1	Inactive	26.1 ± 15.0	19.1 ± 12.5	56.8 ± 1.4	Inactive	21.4 ± 8.4
6b	Inactive	Inactive	Inactive	Inactive	Inactive	Inactive	Inactive
6c	Inactive	Inactive	Inactive	Inactive	Inactive	Inactive	Inactive
6d	19.2 ± 8.9	Inactive	42.0 ± 1.9	9.0 ± 4.7	43.4 ± 9.3	Inactive	32.2 ± 0.1
6e	Inactive	Inactive	23.9 ± 27.8	53.3 ± 7.2	19.5 ± 37.4	Inactive	50.6 ± 3.9
6f	16.6 ± 11.2	55.5 ± 25.4	81.2 ± 0.7	72.6 ± 0.7	81.0 ± 8.5	55.8 ± 30.7	76.1 ± 0.4
6g	Inactive	Inactive	Inactive	Inactive	Inactive	Inactive	Inactive
6h	23.3 ± 2.9	11.6 ± 4.2	16.7 ± 3.7	18.2 ± 7.0	53.1 ± 9.9	16.9 ± 4.9	46.5 ± 4.4
6i	11.0 ± 1.3	29.4 ± 9.8	Inactive	16.7 ± 3.9	56.9 ± 2.7	18.5 ± 4.3	54.2 ± 2.2
6j	40.3 ± 1.9	Inactive	16.3 ± 10.1	12.4 ± 5.0	30.6 ± 11.6	8.9 ± 5.1	33.5 ± 0.4
6k	93.1 ± 7.8	>100	55.2 ± 4.1	90.8 ± 4.5	>100	47.6 ± 2.5	80.3 ± 2.4
6l	Inactive	Inactive	Inactive	Inactive	Inactive	Inactive	Inactive
6m	39.7 ± 12.8	Inactive	19.4 ± 3.6	10.9 ± 5.0	48.9 ± 7.5	Inactive	Inactive
7a	>100	>100	74.2 ± 5.2	38.4 ± 2.7	90.7 ± 4.1	Inactive	55.6 ± 6.6
7b	99.2 ± 5.2	81.1 ± 2.0	86.3 ± 7.7	92.5 ± 6.6	86.4 ± 1.1	55.8 ± 24.1	87.4 ± 1.1
7c	>100	>100	88.6 ± 4.6	>100	>100	94.9 ± 7.9	>100

% Growth inhibition at 20μM

Entry	A549	AsPC1	HT29	MDA-MB-231	PC3	SKOV3	U2OS
7d	13.8 ± 9.8	Inactive	72.4 ± 7.6	50.2 ± 8.9	88.5 ± 1.9	Inactive	46.9 ± 7.4

Table 3

Dose-response growth inhibition study with **7c**.

Cell line	GI$_{50}$ (µM)
A549	6.4 ± 3.0
AsPC1	17.3 ± 0.9
HT29	12.1 ± 7.4
MDA-MB-231	8.4 ± 0.9
PC3	5.9 ± 2.7
SKOV3	16.8 ± 5.2
U2OS	10.8 ± 0.2